DRAFT SF 298

1. Report Date (dd-mm-yy)	2. Report Type	3. Dates covered (from... to)
4. Title & subtitle Bifurcation Based Nonlinear Feedback Control for Rotating Stall in Axial Compressors		5a. Contract or Grant # 5b. Program Element #
6. Author(s)		5c. Project # 5d. Task # 5e. Work Unit #
7. Performing Organization Name & Address		8. Performing Organization Report #
9. Sponsoring/Monitoring Agency Name & Address		10. Monitor Acronym 11. Monitor Report #
12. Distribution/Availability Statement Distribution approved for Public Release, Distribution Unlimited		
13. Supplementary Notes TR downloaded from a WWW unrestricted URL.		
14. Abstract 19970121 156		
15. Subject Terms		

Security Classification of			19. Limitation of Abstract	20. # of Pages	21. Responsible Person (Name and Telephone #)
16. Report Unclass	17. Abstract Unclass	18. This Page Unclass	Unlimited		

Bifurcation Based Nonlinear Feedback Control for Rotating Stall in Axial Compressors *

Guoxiang Gu[§], Andrew Sparks[†] and Siva Banda[†]

April 1996

Abstract

Classical bifurcation analysis for nonlinear dynamics is used to derive a nonlinear feedback control law that eliminates the hysteresis loop associated with rotating stall and extends the stable operating range in axial compressors. The proposed control system employs pressure rise as output measurement and throttle position as actuating signal for which both sensor and actuator exist in the current configuration of axial compressors. Thus, our results provide a practical solution for rotating stall control in axial compressors.

1 Introduction

An axial compressor is a vital part of turbine-based aeroengines. However, the engine performance is effectively reduced by rotating stall and surge in axial compressors, which are instabilities that arise in the unsteady fluid dynamics. One reason that these unsteady aerodynamic instabilities can lead to large penalties in performance is that they are difficult to predict accurately during design. Feedback control has to be employed to suppress the rotating stall and surge in order to extend the stable operating range and/or to enlarge domains of attraction of stable equilibria for compressor systems and to improve the engine performance.

As such, rotating stall and surge control has become an active research field, especially in the past decade due to the emergence of the Moore-Greitzer model [12]. This is a low order nonlinear state-space model that captures the nonlinear dynamics of the compressor system through its bifurcation characteristics [2, 11]. Although initial research has focused on linear control for rotating stall [5, 14], nonlinear control has gradually gained more recognition and attracted more attention. In fact, the application of classical nonlinear dynamics to rotating stall and surge dynamics motivated a simplified approach to rotating stall and surge control based on bifurcation theory. This idea was developed by

*This work was supported in part by AFOSR under contract no. F49620-94-1-0415DEPSCoR, and by WL/FIGC of Wright-Patterson AFB under a Summer Faculty Fellowship grant.

§ Department of Electrical and Computer Engineering, Louisiana State University, Baton Rouge, LA 70803-5901.

† Flight Dynamics Directorate, Wright Laboratory, Wright-Patterson Air Force Base, OH, 45433-7531.

Abed and his co-workers [1, 2, 10, 16] and was shown to be effective for implementation in industrial turbomachinery by Nett and his group [6, 7].

In this paper we pursue a nonlinear control approach based on bifurcation theory. The proposed control system employs pressure rise as output measurement and throttle position as actuating signal for which both sensor and actuator are available in current axial compressors. This is in contrast to the linear control method in [5, 14] that requires 2D (two-dimensional) sensing and 2D actuation, to the nonlinear control method in [10, 16, 6, 7] that requires measurement of amplitude of nonaxisymmetric disturbance flow, or rotating stall, and to the more recent work in [4, 8] that requires air jets as actuators. A nonlinear feedback control law is derived based on classical bifurcation theory for nonlinear dynamics and is shown to be effective in eliminating the hysteresis loop associated with rotating stall and in extending the stable operating range of the compressor characteristic. In comparison with the existing results on nonlinear control of rotating stall, our feedback control law accomplishes the same goal as those reported in [10, 16], and more importantly has the potential for surge control as well.

The schematic diagram of the axial compressor is given in Figure 1. The notations adopted in this paper are consistent with those in [12, 11] with minor changes:

R	=	mean rotor radius	U	=	blade speed at mean radius
A_c	=	compressor duct area	V_p	=	volume of plenum
L_c	=	total geometric length	l_c	=	total aerodynamic length (L_c/R)
a_s	=	speed of sound	p_s	=	static pressure at end of duct and in plenum
B	=	$(U/2a_s)\sqrt{V_p/(A_cLc)}$	p_T	=	total pressure ahead of entrance and
ρ	=	density			following the throttle duct
a	=	time-lag of blade passage	ψ	=	$(p_T - p_T)/\rho U^2$: total-to-static pressure rise
V	=	local flow velocity	ϕ	=	V/U: local flow coefficient at station 0
γ	=	throttle position	φ	=	nonaxisymmetric disturbance in flow coefficient
IGV	=	inlet guide vanes	l_E, l_I, l_T	=	length of exit, entrance, and throttle
ϕ_T	=	flow coefficients in throttle			ducts, in wheel radius
λ	=	exit duct length factor	ξ	=	Ut/R with t time

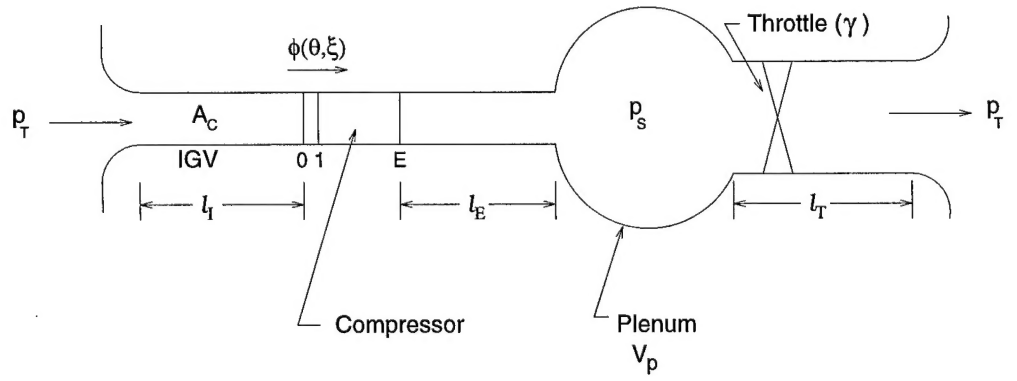

Figure 1: Schematic of compression systems

2 Moore-Greitzer Model and Rotating Stall Control

For the basic compression system shown in Figure 1, the local flow coefficient at station 0 is denoted by $\phi(\xi,\theta)$. The circumferential mean of the flow coefficient at station 0 is denoted by $\overline{\phi}(\xi)$ and is given by

$$\overline{\phi}(\xi) = \frac{1}{2\pi}\int_0^{2\pi} \phi(\xi,\theta)\, d\theta, \implies \phi(\xi,\theta) = \overline{\phi}(\xi) + \varphi_0(\xi,\theta),$$

where $\varphi_0(\xi,\theta) = \varphi(\xi,\theta,0)$ with $\varphi(\xi,\theta,\eta)$ the flow disturbance. If the gas flow is incompressible and irrotational, then there exists a disturbance potential flow $\tilde{\phi}(\xi,\theta,\eta)$ that satisfies Laplace's equation

$$\frac{\partial^2\tilde{\varphi}}{\partial\theta^2} + \frac{\partial^2\tilde{\varphi}}{\partial\eta^2} = 0. \tag{1}$$

The boundary condition is taken as [11]

$$\frac{\partial\tilde{\varphi}}{\partial\eta}(\xi,\theta,-l_F) = 0, \tag{2}$$

where $l_F \geq l_I$. If the disturbance flow potential and circumferential mean of the flow are known, then the pressure rise coefficient $\psi(\xi)$ is determined by the momentum equation [12]:

$$\psi = \psi_c(\phi) - l_c\frac{d\overline{\phi}}{d\xi} - \lambda\frac{\partial\tilde{\varphi}}{\partial\xi}\bigg|_{\eta=0} - \frac{1}{2a}\left(2\frac{\partial^2\tilde{\varphi}}{\partial\xi\partial\eta} + \frac{\partial^2\tilde{\varphi}}{\partial\theta\partial\eta}\right)\bigg|_{\eta=0}. \tag{3}$$

The pressure rise is balanced by the pressure drop in plenum governed by equation:

$$l_c\frac{d\psi}{d\xi} = \frac{1}{4B^2}\left(\overline{\phi} - \phi_T\right) = \frac{1}{4B^2}\left(\overline{\phi} - F_T^{-1}(\psi)\right), \quad \psi = F_T(\phi_T) = \frac{1}{2}K_T\phi_T^2, \tag{4}$$

by assuming a parabolic throttle characteristic. For uniform and steady flow, $\psi = \psi_c$, the performance characteristic given by [12]

$$\psi_c(\phi) = H\left[c_0 + c_1\left(\frac{\phi}{W} - 1\right) + c_3\left(\frac{\phi}{W} - 1\right)^3\right]. \tag{5}$$

Laplace's equation in (1) with the boundary condition in (2) yield the harmonic form for disturbance potential flow [11, 1] as follows:

$$\tilde{\varphi} = \sum_{n=1}^{\infty}\left(a_n(\xi)e^{jn\theta} + \bar{a}_n(\xi)e^{-jn\theta}\right)\left(e^{n(\eta+l_F)} + e^{-n(\eta+l_F)}\right), \quad \eta \leq 0. \tag{6}$$

Thus the flow disturbance at station 0 has the form

$$\varphi_0 = \sum_{n=1}^{\infty}\varphi_{0n}, \quad \varphi_{0n} = 2WA_n(\xi)\sin(n\theta - r_n\xi), \quad A_n = 2n|a_n|\sinh(nl_F)/W \tag{7}$$

with r_n a constant by assuming constant speed of the nth harmonic disturbance flow, i.e., constant wave speed. The value of l_F can be taken as infinity provided A_n has a finite value. Using first order

approximation, or single harmonic Galerkin method for flow disturbance, Moore and Greitzer obtained the following nonlinear state-space model [12]:

$$\frac{d\psi}{d\xi} = \frac{W/H}{4B^2}\left[\frac{\overline{\phi}}{W} - \frac{1}{W}F_T^{-1}(\psi)\right]\frac{H}{l_c}, \tag{8}$$

$$\frac{d\overline{\phi}}{d\xi} = \left[-\frac{\psi}{H} + c_0 + \left(c_1 + 6c_3A^2\right)\left(\frac{\overline{\phi}}{W} - 1\right) + c_3\left(\frac{\overline{\phi}}{W} - 1\right)^3\right]\frac{H}{l_c}, \tag{9}$$

$$\frac{dA}{d\xi} = A\left(\left[1 - \left(\frac{\overline{\phi}}{W} - 1\right)^2 - A^2\right]\frac{3aH}{2W}\right)\left(1 + \frac{a\lambda}{n}\tanh(nl_F)\right)^{-1}, \tag{10}$$

for compression systems.

If the following changes of variables:

$$\Phi = \frac{\overline{\phi}}{W} - 1, \quad \Psi = \frac{\psi}{H}, \quad \tau = \frac{H}{Wl_c}\xi, \tag{11}$$

are used, and with notations $\beta = 2BH/W$, $\gamma = \sqrt{2H/K_T}/W$, and $\sigma = 1.5al_c/(1+a\lambda\tanh(l_F)/n)$, then (8) – (10) are converted into the following simpler form of ODEs [11]:

$$\dot{\Psi} = \frac{1}{\beta^2}\left(\Phi - \Phi_\gamma(\Psi)\right), \qquad \Phi_\gamma(\Psi) = \gamma\sqrt{\Psi} - 1, \ \gamma > 0, \tag{12}$$

$$\dot{\Phi} = -\Psi + \Psi_c(\Phi) + 6c_3\Phi A^2, \quad \Psi_c(\Phi) = c_0 + c_1\Phi + c_3\Phi^3, \tag{13}$$

$$\dot{A} = \sigma A\left(1 - \Phi^2 - A^2\right), \qquad \sigma > 0, \tag{14}$$

where $\dot{x}$ denotes derivative of x with respect to "time" variable τ. The throttle position γ[1] and parameter β play an important role in the dynamics of axial compressors. The cubic polynomial Ψ_c is compressor dependent. In [13], the following values

$$c_0 = 8/3, \ \ c_1 = 1.5, \ \ c_3 = -0.5, \tag{15}$$

are assumed, while in reality these coefficients are uncertain. It should be clear that a cubic curve is completely parameterized by W, H, and c_0, with $c_1 = -3c_3 = 1/2$, that define its shape and position. In this paper, we adopt an approach that the variation of H is translated into those for c_0, c_1, and c_3. We are thus led to the following assumption:

$$1 < c_0 < 5, \quad c_1 > 0, \quad c_3 < 0 \quad \text{and} \quad c_1 + 3c_3 = 0, \tag{16}$$

for the coefficients of the performance characteristic curve. The parameter σ is less important and less interesting.

There are two sets of equilibrium points. The first set is $A_e = 0$ corresponding to the axisymmetric flow. In this case the compressor performance characteristic is given by

$$\Psi_e = \Psi_c(\Phi_e) = c_0 + c_1\Phi_e + c_3\Phi_e^3 \tag{17}$$

[1]Throttle position can be implemented with bleedvalves if used as actuator.

shown by solid curve on the upper-right part of Figure 2 that extends to the left with dotted line. The steady operating point of the compressor is determined by the intersection of the performance characteristic $\Psi_e = \Psi_c(\Phi_e)$ and the throttle characteristic

$$\Phi_e = \Phi_\gamma(\Psi_e) \iff \Psi_e = \frac{1}{\gamma^2}(1+\Phi_e)^2$$

shown with two dashed lines corresponding to two different γ values. See points A and D in Figure 2. The second set of equilibrium points is given by $A_e \neq 0$ where A_e represents the amplitude of the nonaxisymmetric disturbance flow, or rotating stall. In this case, the performance characteristic is degenerated into the rotating stall characteristic

$$\Psi_e = \Psi_s(\Phi_e) = c_0 + (c_1 + 6c_3)\Phi_e - 5c_3\Phi_e^3 \tag{18}$$

shown by solid curve on the lower-left part of Figure 2 that extends with a sharp slope to the right indicated by dotted line.

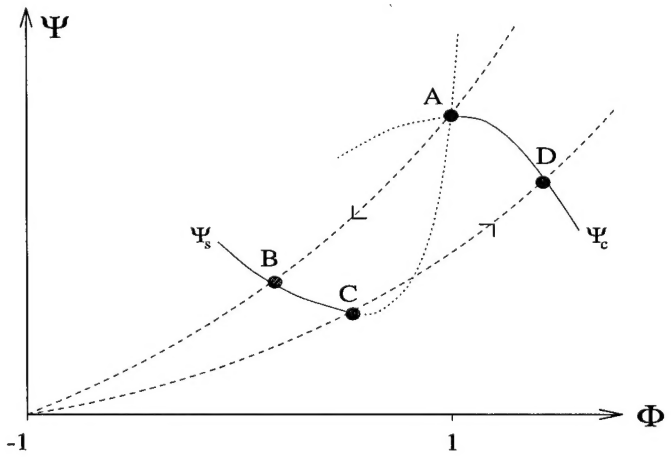

Figure 2: Schematic of compressor characteristic

By employing a linearization method, it can be easily shown that the solid parts of Ψ_c and Ψ_s are stable, but dotted parts of Ψ_c and Ψ_s are unstable. Thus, if one gradually decreases the throttle position γ that initially determines the operating point D, then the steady operating point moves along curve Ψ_c to point A, the peak of the compressor performance characteristic curve. Further analysis with center manifold theorem for nonlinear dynamics [15] indicates that point A is unstable if (15) is used for Ψ_c as in (17). Thus nonaxisymmetric disturbance flow, or rotating stall, will eventually be born and the steady operating condition will quickly settle at point B on the rotating stall characteristic curve Ψ_s. There is a substantial drop in both the pressure rise and flow coefficient. At this momemt, however, increasing the throttle position does not recover axisymmetric flow. Rather, the operating point moves along curve Ψ_s, resulting in even lower pressure rise. It then settles quickly at point D of the performance characteristic curve Ψ_c after reaching point C. The described process represented by D-A-B-C-D in Figure 2 constitutes the hysteresis loop associated with rotating stall. Because the

compressor has to work under much lower pressure rise and flow coefficients when rotating stall occurs, prolonged operation under this condition will cause severe stress and overheating in rotor blades, and may thus damage the aeroengine. However little can be done to return to axisymmetric flow once rotating stall is fully developed. The only remedy at present is to shut down the engine and restart it.

Rotating stall in axial compressors poses a great challenge to both turbomachinery engineers and control engineers. Because of the existence of rotating stall, large stall margins have to be employed so that axial compressors can only operate at much lower pressure rise but higher flow coefficient than point A, resulting in poor engine performance; because of the existence of hysteresis loop, active control may not be effective once rotating stall is fully developed. It is perhaps beneficial to look into the dependence of equilibrium point (Ψ_e, Φ_e, A_e) on the throttle position γ, and to understand how local stability changes with respect to γ. Recall that the throttle position synthesizes the effects of combustion chamber, bleedvalves, and disturbances to the flow in compressors. Thus it is a highly uncertain parameter and very sensitive to inlet disturbance.

By setting the right hand side of (12) – (14) to zero, there hold

$$\gamma^2 = \frac{(\Phi_e + 1)^2}{\Psi_c(\Phi_e)}, \quad \text{for } A_e = 0, \text{ all } \Phi_e, \text{ and} \tag{19}$$

$$\gamma^2 = \frac{(\Phi_e + 1)^2}{\Psi_s(\Phi_e)}, \quad \text{for } A_e \neq 0, \ \Phi_e = \sqrt{1 - A_e^2}. \tag{20}$$

Thus equilibrium solution bifurcates at

$$\gamma = \gamma_c = \frac{2}{\sqrt{c_0 + c_1 + c_3}}, \ A_e = 0, \ \Phi_e = 1, \ \Psi_e = c_0 + c_1 + c_3. \tag{21}$$

That is, more than one equilibrium solution is born at $\gamma = \gamma_c$. Because these bifurcated solutions are independent of time, they are called stationary bifurcation, and their stability can be determined using the well-known linearization method. Clearly rotating stall occurs at $A_e \neq 0$ that is also a function of γ. Thus stability of A_e is hinged to the values of γ and shown by the bifurcation diagram (A_e, γ) as in (a) of Figure 4 at the end of Section 4, where (15) is used for the performance characteristic curve Ψ_c as in (17). Again by convention, the solid part corresponds to stability and dotted part instability. In light of [9], this is exactly the subcritical pitchfork bifurcation and is well known for causing the hysteresis loop in classical bifurcation theory. It is interesting to note that the hysteresis loop persists as long as $c_0 < 5$, but disappears for $c_0 > 5$ because of the change of pitchfork bifurcation from subcritical into supercritical. This fact was pointed out by McCaughan [11]. A more interesting observation made by Wang and Abed [16] for the case of $c_0 < 5$ is the loss of stabilizability with linear feedback at bifurcation point $\gamma = \gamma_c$. Indeed, setting $\gamma = \gamma_c + u$, and linearizing the Moore-Greitzer model at (Ψ_e, Φ_e, A_e), $A_e = 0$, yield the linearized model

$$\begin{bmatrix} \dot{x}_1 \\ \dot{x}_2 \\ \dot{x}_3 \end{bmatrix} = \begin{bmatrix} -\beta^{-2}\Psi'_{\gamma_c}(\Psi_e) & \beta^{-2} & 0 \\ -1 & \Psi'_c(\Phi_e) & 0 \\ 0 & 0 & \sigma\left(1 - \Phi_e^2\right) \end{bmatrix} \begin{bmatrix} x_1 \\ x_2 \\ x_3 \end{bmatrix} + \begin{bmatrix} -\beta^{-2}\Psi'_{\gamma_c}(\Psi_e) \\ 0 \\ 0 \end{bmatrix} u, \tag{22}$$

where $x_1 = \Psi - \Psi_e$, $x_2 = \Phi - \Phi_e$, and $x_3 = A$. Clearly for $|\Phi_e| \leq 1$, the unstable eigenvalue at $\sigma(1 - \Phi_e^2)$ is not affected by linear control. Thus if the throttle position is used as actuator, linear control fails utterly. This observation motivated Liaw and Abed [10], and Wang and Abed [16] to use the nonlinear feedback control law $u = kA^2$ based on bifurcation theory. They demonstrated that the nonlinear feedback gain k can be chosen such that the pitchfork bifurcation can be altered from subcritical into supercritical, thereby stabilizing the bifurcation point $\gamma = \gamma_c$ and $A_e > 0$, and eliminating the hysteresis loop associated with rotating stall.

While the nonlinear control law in [10, 16] was experimentally validated in [3, 7], it remains unclear how A, the amplitude of nonaxisymmetric disturbance flow, can be measured. One probably has to measure local flow coefficient ϕ around the circumference of the compressor in order to estimate A. 2D sensing is thus required especially when high order harmonics are involved. At present, hot wires are used for measurement of local flow coefficient [14]. These are very delicate devices, making it difficult for them to survive the hostile environment of aeroengines. Rather, pressure transducers are more reliable and endurable in the volatile flow field. In addition it is less likely for the control law $u = kA^2$ to be effective for surge control, especially for the case of pure surge that is in contrast to the potential nonlinear control law $u = \mathcal{N}(\Psi)$. Therefore a challenging problem is the design of a nonlinear feedback control system where pressure rise is used as output measurement and throttle position as actuating signal. It should be clear that such a control system requires only 1D sensing and 1D actuation even if high order harmonics are involved. Moreover both pressure sensor and throttle actuator are available in current configuration of axial compressors. The difficulty lies in the design of nonlinear feedback control law that achieves the same results as in [10, 16, 3]. This will be studied in next section.

3 Nonlinear Feedback Control Based on Bifurcation Theory

This section focuses on the design of a nonlinear feedback control system where pressure transducer is used as sensor and throttle as actuator. As discussed earlier, linear control fails to stabilize the equilibria of $A_e \geq 0$ for the case $c_0 < 5$. Thus nonlinear feedback control law has to be employed. We begin our discussion with the geometric shape of the bifurcation diagram in (a) of Figure 4. The bifurcated solution, according to (19), can be written as $\gamma = \gamma(A_e)$ for $A_e \geq 0$ at least locally. The hysteresis loop associated with subcritical pitchfork bifurcation is due to the two maximum values of $\gamma(A_e)$ at $A_e \neq 0$, whereas supercritical pitchfork bifurcation admits only one maximum value for $\gamma(A_e)$ that occurs at $A_e = 0$. Intuitively speaking, the elimination of the hysteresis loop in (a) of Figure 4 is hinged to the elimination of the two extreme values of $\gamma(A_e)$ at $A_e \neq 0$, or merging them into a single one located at $A_e = 0$. The nonlinear feedback control law proposed in [10, 16] accomplishes exactly this goal.

For the control system considered in this paper, the nonlinear feedback law $u = \mathcal{N}(\Psi)$ is employed where $\mathcal{N}(\cdot)$ is a memoryless nonlinear function. The goal is to design $\mathcal{N}(\cdot)$ such that it eliminates the hysteresis loop associated with rotating stall and stabilizes the equilibria of $A_e \neq 0$. Substituting

$\gamma = \gamma_o + \mathcal{N}(\Psi)$ into (12) yields

$$\dot{\Psi} = \frac{1}{\beta^2}\left(\Phi + 1 - \mathcal{N}(\Psi)\sqrt{\Psi} - \gamma_o\sqrt{\Psi}\right), \tag{23}$$

where γ_o is the normal value of the throttle position that may not be the same as γ_c, the critical value at bifurcation. It follows that the nonlinear feedback control law $u = \mathcal{N}(\Psi)$ changes the throttle characteristic curve that is obtained by setting the right hand side of (23) to zero, yielding

$$(\gamma_c + \mathcal{N}(\Psi_e))^2\,\Psi_e = (1 + \Phi_e)^2.$$

In general the steady pressure rise Ψ_e is not a single-valued function of Φ_e unless

$$u = \mathcal{N}(\Psi_e) = K/\sqrt{\Psi} \tag{24}$$

is chosen with K the feedback gain to be designed. It should be pointed out that although the throttle characteristic is changed for $K \neq 0$, the compressor performance characteristic Ψ_c and rotating stall characteristic Ψ_s remain the same. We will derive an explicit expression of K that eliminates the hysteresis loop associated with rotating stall, and stabilizes the equilibria for $A_e \neq 0$ under some mild conditions. For this purpose, setting the right hand side of (13), (14), and (23) to zero gives the expression

$$\gamma_o^2 = \frac{(\Phi_e + 1 - K)^2}{\Psi_c(\Phi_e)}, \qquad \text{for } A_e = 0, \text{ all } \Phi_e, \text{ and} \tag{25}$$

$$\gamma_o^2 = \frac{(\Phi_e + 1 - K)^2}{\Psi_s(\Phi_e)}, \qquad \text{for } A_e \neq 0, \ \Phi_e = \sqrt{1 - A_e^2}. \tag{26}$$

These two equations reduce to (19) and (20) respectively for $K = 0$ and $\gamma_o = \gamma$. We will first demonstrate how introduction of nonlinear feedback gain K as in (24) can actually change the geometric shape of the subcritical pitchfork bifurcation in (a) of Figure 4.

Theorem 3.1 *Suppose the coefficients of Ψ_c as in (17) satisfy (16), and $c_0 > -4c_3$. If the nonlinear feedback gain in (24) is chosen as*

$$K = \frac{2(c_0 + 10c_3)}{9c_3 - c_1}, \tag{27}$$

then $\gamma_o = \gamma_o(A_e)$, obtained from (26), admits only one extreme value for $-1 \leq A_e \leq 1$, and it takes place at $A_e = 0$.

Proof: For $A_e \neq 0$ as in (26), direct calculation for derivative of γ_o^2 with respect to A_e yields

$$\frac{d\gamma_o^2}{dA_e} = 2\gamma_o \frac{d\gamma_o}{d\Phi_e}\frac{d\Phi_e}{dA_e} = \left(\frac{-A_e}{\sqrt{1 - A_e^2}}\right)\frac{d\gamma_o^2}{d\Phi_e}.$$

Thus, there holds

$$\gamma_o'(A_e) := \frac{d\gamma_o}{dA_e} = -\frac{A_e}{2\gamma_o\Phi_e}\frac{d\gamma_o^2}{d\Phi_e} = -\frac{A_e}{2\Phi_e\Psi_s(\Phi_e)}F(\Phi_e), \tag{28}$$

where $\Phi_e = \sqrt{1 - A_e^2}$, and $F(\Phi_e)$ is given by

$$F(\Phi_e) = 2\Psi_s(\Phi_e) - \Psi_s'(\Phi_e)(\Phi_e + 1 - K). \tag{29}$$

It is claimed that $F(\Phi_e) > 0$ for $0 \leq \Phi_e < 1$ provided that K satisfies (27). Indeed, there holds

$$f(\Phi_e) = \frac{dF(\Phi_e)}{d\Phi_e} = \Psi_s'(\Phi_e) - (\Phi_e + 1 - K)\Psi_s''(\Phi_e) = -30c_3\Phi_e\left(K - 1 - \frac{1}{2}\Phi_e - \frac{(c_1 + 6c_3)}{30c_3\Phi_e}\right).$$

Thus for $c_3 < 0$ and $c_1 + 6c_3 = 3c_3 < 0$ by $c_1 = -3c_3$ as assumed in (16),

$$\frac{1}{2}\Phi_e + \frac{(c_1 + 6c_3)}{30c_3\Phi_e} \geq \sqrt{\frac{c_1 + 6c_3}{15c_3}} \geq 0$$

for all $\Phi_e \geq 0$. Moreover the gain K chosen as in (27) satisfies

$$K = \frac{2(c_0 + 10c_3)}{9c_3 - c_1} = \frac{c_0 + 10c_3}{6c_3} < 1$$

by $c_0 > -4c_3$ and $c_3 < 0$. It follows that

$$K - 1 - \frac{1}{2}\Phi_e - \frac{(c_1 + 6c_3)}{30c_3\Phi_e} \leq K - 1 - \sqrt{\frac{c_1 + 6c_3}{15c_3}} = K - 1 - \frac{1}{\sqrt{5}} < 0, \tag{30}$$

using the hypothesis $c_1 + 3c_3 = 0$. By again $c_3 < 0$, the above inequality leads to the conclusion that for all $\Phi_e > 0$,

$$f(\Phi_e) = \frac{dF(\Phi_e)}{d\Phi_e} = -30c_3\Phi_e\left(K - 1 - \frac{1}{2}\Phi_e - \frac{(c_1 + 6c_3)}{30c_3\Phi_e}\right) < 0.$$

Evaluating $F(\Phi_e)$ at $\Phi_e = 1$ gives, using (27),

$$F(\Phi_e = 1) = 2c_0 + 20c_3 + K(c_1 - 9c_3) = 0.$$

Since $f(\Phi_e) = F'(\Phi_e) < 0$ for all $\Phi_e > 0$, $F(\Phi_e)$ is a strictly decreasing function of Φ_e, and since $F(\Phi_e = 1) = 0$, we conclude that

$$F(\Phi_e) = F\left(\sqrt{1 - A_e^2}\right) > 0, \ \forall A_e = \sqrt{1 - \Phi_e^2} > 0,$$

by $\Phi_e = \sqrt{1 - A_e^2}$. The above inequality in turn implies that

$$\gamma_o'(A_e) = \frac{d\gamma_o}{dA_e} \begin{cases} > 0, & \text{for } A_e < 0, \\ < 0, & \text{for } A_e > 0, \end{cases}$$

by $\gamma_o > 0$, $\Phi_e > 0$ according to (28). Thus $\gamma_o'(A_e) = 0$ if and only if $A_e = 0$ that is the only extreme point for the function $\gamma_o(A_e)$, in fact, a maximum point, in the interval $|A_e| \leq 1$. ∎

The hypothesis on the coefficients of the performance characteristic curve Ψ_c as in (16) is reasonable. Typically, $c_1 = 1.5$ and $c_3 = -0.5$. For the compressor model as in [13], $c_0 = 8/3$. Thus. the feedback back gain in (27) is obtained as

$$K = \frac{2(c_0 + 10c_3)}{9c_3 - c_1} = \frac{7}{9} < 1,$$

as required. In fact by examing the proof, $K < 1$ is not a necessary condition for the result in Theorem 3.1 to hold. Indeed, (30) indicates that $K < 1$ can be improved to $K < 1 + \sqrt{3/15} = 1.4472$. Because (30) ensures $f(\Phi_e) < 0$ for all $\Phi_e \geq 0$, $K < 1.4472$ is again not a necessary condition. This will be demonstrated in the simulation section. However because large K implies aggressive control strategy, and consequently causes more distortion to the throttle characteristic, we will restrict our development to the scope confined by $0 < K < 1$ in the rest of the section.

A more fundamental question on the nonlinear feedback gain as given in (27), is whether or not it stabilizes the bifurcated solution at $\gamma_o \leq \gamma_c$, and $A_e \geq 0$, excluding the equilibria $A_e \equiv 0$. We will consider first the equilibrium point $A_e = 0$ at critical value of γ_o.

Theorem 3.2 *Suppose that the coefficients of the performance characteristic curve Ψ_c satisfy (16), and in addition*

$$c_0 > -4c_3, \quad c_3 \leq -1/2. \tag{31}$$

If the nonlinear feedback gain K is chosen as

$$K = \max\left\{2 - \frac{1}{3}(c_0 + c_1 + c_3), \frac{2(c_0 + 10c_3)}{9c_3 - c_1}\right\}. \tag{32}$$

Then $0 < K < 1$, and the equilibrium point $A_e = 0$ at

$$\gamma_o = \frac{\Phi_e + 1 - K}{\sqrt{\Psi_e}} = \frac{2 - K}{\sqrt{c_0 + c_1 + c_3}} \tag{33}$$

is asymptotically stable.

Proof: The conditions (16) and (31) imply that

$$c_0 + c_1 + c_3 = c_0 - 2c_3 > -6c_3 \geq 3, \quad \frac{2(c_0 + 10c_3)}{9c_3 - c_1} = \frac{-c_0 - 10c_3}{-6c_3} \leq \frac{4c_3 - 10c_3}{-6c_3} = 1. \tag{34}$$

Thus (16) and (31) ensure that the gain chosen as in (32) satisfies $0 < K < 1$. Since $u = K/\sqrt{\Psi}$, the nonlinear feedback system has the form

$$\begin{bmatrix} \dot{x}_1 \\ \dot{x}_2 \\ \dot{x}_3 \end{bmatrix} = \begin{bmatrix} -\frac{\gamma_o}{2\beta^2\sqrt{\Psi_e}} & \beta^{-2} & 0 \\ -1 & \frac{3}{2}(1 - \Phi_e^2) & 0 \\ 0 & 0 & \sigma\,(1 - \Phi_e^2) \end{bmatrix} \begin{bmatrix} x_1 \\ x_2 \\ x_3 \end{bmatrix} + \text{ higher order terms}, \tag{35}$$

where $x_1 = \Psi - \Psi_e$, $x_2 = \Phi - \Phi_e$, and $x_3 = A$. Because the equilibrium solution bifurcates at $\Phi_e = 1$, the critical value of γ_o satisfies (33). Thus center manifold theorem [15] can be applied to determine the stability of $A_e = 0$ at γ_o. For this purpose, set

$$\begin{bmatrix} x_1 \\ x_2 \end{bmatrix} = \begin{bmatrix} \alpha_1 \\ \alpha_2 \end{bmatrix} x_3^2 + \begin{bmatrix} \beta_1 \\ \beta_2 \end{bmatrix} x_3^3 + \mathcal{O}(x_3^4). \tag{36}$$

Then by $\Phi_e = 1$,

$$\dot{x}_3 = \dot{A} = -\sigma A^3 - 2\sigma(\Phi - 1)A + \mathcal{O}(A^4) = -\sigma x_3^3 - 2\sigma x_2 x_3 + \mathcal{O}(x_3^4) = \mathcal{O}(x_3^3).$$

Thus there holds

$$\begin{bmatrix} \dot{x}_1 \\ \dot{x}_2 \end{bmatrix} = \begin{bmatrix} 2\alpha_1 x_3 + 3\beta_1 x_3^2 \\ 2\alpha_2 x_3 + 3\beta_2 x_3^2 \end{bmatrix} \dot{x}_3 = \begin{bmatrix} 2\alpha_1 x_3 + 3\beta_1 x_3^2 \\ 2\alpha_2 x_3 + 3\beta_2 x_3^2 \end{bmatrix} \mathcal{O}(x_3^3) = \mathcal{O}(x_3^4).$$

On the other hand, the nonlinear feedback system in (12)–(14), in conjunction with (24), yield

$$\begin{aligned} \begin{bmatrix} \dot{\Psi} \\ \dot{\Phi} \end{bmatrix} &= \begin{bmatrix} \dot{x}_1 \\ \dot{x}_2 \end{bmatrix} = \begin{bmatrix} -\frac{\gamma_o}{2\beta^2\sqrt{\Psi_e}} & \beta^{-2} \\ -1 & 0 \end{bmatrix} \begin{bmatrix} x_1 \\ x_2 \end{bmatrix} - 3 \begin{bmatrix} 0 \\ x_3^2 \end{bmatrix} + \cdots \\ &= \begin{bmatrix} -\frac{\gamma_o}{2\beta^2\sqrt{\Psi_e}} & \beta^{-2} \\ -1 & 0 \end{bmatrix} \begin{bmatrix} \alpha_1 x_3^2 + \beta_1 x_3^3 \\ \alpha_2 x_3^2 + \beta_2 x_3^3 \end{bmatrix} - 3 \begin{bmatrix} 0 \\ x_3^2 \end{bmatrix} + \mathcal{O}(x_3^4), \end{aligned}$$

by (36). Consequently the coefficients of lower order terms x_3^k for $k \leq 3$ are zero that results in

$$\beta_1 = \beta_2 = 0, \quad \alpha_1 = -3, \quad \alpha_2 = -\frac{3\gamma_o}{2\sqrt{\Psi_e}}. \tag{37}$$

It follows that

$$\dot{x}_3 = -\sigma x_3^3 - 2\sigma x_2 x_3 + \mathcal{O}(x_3^4) = -\sigma x_3^3 - 2\sigma x_3(\alpha_2 x_3^2) + \mathcal{O}(x_3^4) = -\sigma(1 + 2\alpha_2)x_3^3 + \mathcal{O}(x_3^4). \tag{38}$$

Direct calculation shows that, by substituting the expression for K as in (27),

$$\begin{aligned} 1 + 2\alpha_2 &= \frac{\Psi_e - 6 + 3K}{\Psi_e} \geq \frac{2c_3(\Psi_e - 1) + c_0}{2c_3} \\ &\geq -\frac{2c_3(\Psi_e - 1) + c_0}{\Psi_e} \geq \frac{\Psi_e - 1 - c_0}{\Psi_e} = \frac{c_1 + c_3 - 1}{\Psi_e} \geq 0, \end{aligned}$$

due to $c_3 \leq -1/2$, $c_1 = -3c_3$, and $\Psi_e = \Psi_c(\Phi_e) = c_0 + c_1 + c_3$. For $K = 2 - (c_0 + c_1 + c_3)/3 = 2 - \Psi_e/3$ at $\Phi_e = 1$,

$$1 + 2\alpha_2 = \frac{\Psi_e - 6 + 3K}{\Psi_e} = 0.$$

Hence with K as in (32), $1 + 2\alpha_2 \geq 0$. There are two different cases to consider. Case 1: $1 + 2\alpha_2 > 0$. Then the local asymptotic stability of x_3 is easily concluded by the center manifold theorem in light of (38). Case 2: $1 + 2\alpha_2 = 0$. In this case,

$$\alpha_2 = -\frac{1}{2}, \quad \Longrightarrow \quad \frac{\gamma_o}{\sqrt{\Psi_e}} = \frac{1}{3}$$

by (37). Hence in order to determine the stability of ODE in (38), higher order terms are needed. Now (36) gives

$$\begin{bmatrix} x_1 \\ x_2 \end{bmatrix} = \begin{bmatrix} \alpha_1 \\ \alpha_2 \end{bmatrix} x_3^2 + \begin{bmatrix} a_1 \\ a_2 \end{bmatrix} x_3^4 + \begin{bmatrix} b_1 \\ b_2 \end{bmatrix} x_3^5 + \mathcal{O}(x_3^6), \quad \alpha_1 = -3, \ \alpha_2 = -\frac{1}{2}.$$

Similar calculations shows that

$$\dot{x}_1 = \frac{1}{\beta^2}\left[\left(a_2 - \frac{1}{6}a_1 + \frac{3}{8\Psi_e}\right)x_3^4 + \left(b_2 - \frac{1}{6}b_1\right)x_3^5\right] + \mathcal{O}(x_3^6) = \mathcal{O}(x_3^6), \tag{39}$$

$$\dot{x}_2 = -\left(a_1 - \frac{9}{8}\right)x_3^4 - b_1 x_3^5 + \mathcal{O}(x_3^6) = \mathcal{O}(x_3^6), \tag{40}$$

$$\dot{x}_3 = -\sigma\left(2a_2 + \frac{1}{4}\right)x_3^5 + \mathcal{O}(x_3^6) = \mathcal{O}(x_3^5). \tag{41}$$

Hence, we obtain

$$b_1 = b_2 = 0, \quad a_1 = \frac{9}{8}, \quad a_2 = \frac{a_1}{6} - \frac{3}{8\Psi_e} = \frac{3}{16} - \frac{3}{8\Psi_e}.$$

It follows that

$$2a_2 + \frac{1}{4} = \frac{5}{8} - \frac{3}{4\Psi_e} = \frac{5\Psi_e - 6}{8\Psi_e} > 0$$

by $\Psi_e = c_0 + c_1 + c_3 > 3$ as shown in (34). Thus the ODE in (41) is asymptotically stable, that in turn implies the asymptotic stability of $A_e = 0$ by center manifold theorem. ∎

The condition $c_3 \leq -1/2$ and $c_0 + c_1 + c_3 > 3$ as in (31) is true for the compressor used in [13]. In the case $1 + 2\alpha_2 = 0$, it is advised to choose $\delta > 0$ such that

$$K = \max\left\{2 - \frac{1}{3}(c_0 + c_1 + c_3), \frac{2(c_0 + 10c_3)}{9c_3 - c_1}\right\} + \delta < 1.$$

Such a choice of K makes $1+2\alpha_2 > 0$ that validates the ODE (38) when using center manifold theorem, rather than (41). This is due to the fact that for $1 + 2\alpha_2 = 0$, the bifurcated solution $\gamma_o = \gamma_o(A_e)$ in the neighborhood of $A_e = 0$ has its derivatives

$$\frac{d^i\gamma_o}{dA_e^i}(0) = 0, \quad i = 1, 2, 3.$$

Thus the curve $\gamma_o = \gamma_o(A_e)$ is very flat at $A_e = 0$. Consequently small perturbation of γ_o may cause large variation in A_e that is not desirable. But if $1+2\alpha_2 > 0$, then $\gamma_o''(0) \neq 0$, minimizing the sensitivity of A_e with respect to γ_o in the neighborhood of $A_e = 0$.

The next result is on the local stability of $A_e \neq 0$, but close to $A_e = 0$ when feedback gain K as in (27) is used.

Theorem 3.3 *Suppose that the coefficients of the performance characteristic curve Ψ_c satisfy (16), and (31). If the nonlinear feedback gain K is chosen as in (32), then the equilibrium point $A_e \neq 0$ is asymptotically stable provided A_e is sufficiently close to $A_e = 0$.*

Proof: Projection method as in [9] can be used to show the local stability of the bifurcated solution. We shall, however, employ a more elementary proof that uses no more than linearization method. Indeed, linearization with $x_1 = \Psi - \Psi_e$, $x_2 = \Phi - \Phi_e$, and $x_c = A - A_e$ yields approximate linear system:

$$\begin{bmatrix} \dot{x}_1 \\ \dot{x}_2 \\ \dot{x}_3 \end{bmatrix} = \begin{bmatrix} -\frac{\gamma_o}{2\beta^2\sqrt{\Psi_e}} & \beta^{-2} & 0 \\ -1 & 3c_3A_e^2 + c_1 + 3c_3 & 12c_3A_e\Phi_e \\ 0 & -2\sigma A_e\Phi_e & -2\sigma A_e^2 \end{bmatrix} \begin{bmatrix} x_1 \\ x_2 \\ x_3 \end{bmatrix}.$$

The corresponding characteristic equation is given by

$$\begin{aligned} \lambda^3 &+ \left[\frac{\gamma_o}{2\beta^2\sqrt{\Psi_e}} + (2\sigma - 3c_3)A_e^2 - (c_1 + 3c_3)\right]\lambda^2 \\ &+ \left[\frac{\gamma_o(2\sigma - 3c_3)A_e^2}{2\beta^2\sqrt{\Psi_e}} + 3\sigma\left(8c_3 - 10c_3A_e^2\right)A_e^2 + \frac{1}{\beta^2} - \left(\frac{\gamma_o}{2\beta^2\sqrt{\Psi_e}} + 2\sigma A_e^2\right)(c_1 + 3c_3)\right]\lambda \\ &+ \frac{2\sigma A_e^2}{\beta^2} + \frac{\sigma\gamma_o}{2\beta^2\sqrt{\Psi_e}}\left[3\left(8c_3 - 10c_3A_e^2\right)A_e^2 - 2(c_1 + 3c_3)A_e^2\right] = 0. \end{aligned}$$

As $A_e \to 0$, all the coefficients of the characteristic equation are strictly positive except the constant term that goes to zero. Thus in light of Routh-Hurwitz's stability test, the local stability of the bifurcated solution close to $A_e = 0$ is hinged to the strict positivity of the constant term. Since $c_1 + 3c_3 = 0$, the constant term is

$$\begin{aligned} \frac{2\sigma A_e^2}{\beta^2} + \frac{3\sigma\gamma_o}{2\beta^2\sqrt{\Psi_e}}\left(8c_3 - 10c_3A_e^2\right)A_e^2 &> \frac{2\sigma A_e^2}{\beta^2}\left(1 + \frac{6\gamma_o c_3}{\sqrt{\Psi_e}}\right) \geq \frac{2\sigma A_e^2}{\beta^2}\left(1 - \frac{3\gamma_o}{\sqrt{\Psi_e}}\right) \\ &> \frac{2\sigma A_e^2(3K-6) + (c_0 + c_1 + c_3)}{c_0 + c_1 + c_3} \geq 0, \end{aligned}$$

by $c_1 + 3c_3 = 0$, and $\gamma_o < (2-K)/\sqrt{\Psi_e}$, $\Psi_e < c_0 + c_1 + c_3$ as $\Phi_e < 1$ for $A_e \neq 0$. This concludes the local asymptotic stability of the bifurcated solution near $A_e = 0$. ∎

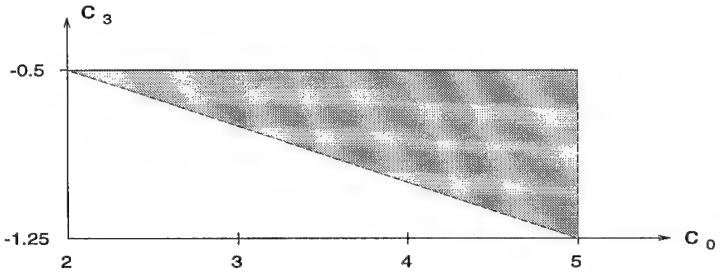

Figure 3: Allowable region for coefficients of compressor characteristic curve

Remark 1: The conditions in Theorems 3.1, 3.2, and 3.3 amount to the following:

$$\text{(i) } c_0 < 5, \quad \text{(ii) } c_3 \leq -0.5, \quad \text{(iii) } c_0 > -4c_3, \tag{42}$$

by $c_1 + 3c_3 = 0$. The condition $c_0 < 5$ indicates the existence of hysteresis loop associated with rotating stall for axial compressors [11]. If $c_0 \geq 5$, nonlinear feedback control is unnecessary. The conditions (ii) and (iii) ensure the existence of the nonlinear feedback law as in (24), such that $0 < K < 1$ that changes the pitchfork bifurcation from subcritical into supercritical, and stabilizes the rotating stall characteristic locally. In fact, in light of the projection method as in ([9]), our nonlinear feedback law stabilizes the bifurcated solution $A_e \neq 0$ for all $0 < \Phi_e < 1$. This is due to the fact that the bifurcated solution $\gamma_o = \gamma_o(A_e)$ does not admit a turning point for $\Phi_e > 0$. The conditions in (42) are represented by shaded area, excluding the dashed side, in Figure 3. If c_0 and c_3 fall into the shaded area, then there exists a stabilizing feedback gain K that can be computed according to (32).

Remark 2: As discussed earlier, $K < 1$ can be improved to $K = K_{\max}$ for some $K_{\max} \geq 1 + 1/\sqrt{5}$ for which Theorem 3.1 still holds. If local stability at $A_e = 0$ and $\Phi_e = 1$ is the only concern as in [10, 16], then the feedback gain in (32) can be replaced by

$$K \geq K_{\min} = 2 - \frac{c_0 + c_1 + c_3}{3}, \tag{43}$$

by the proof of Theorem 3.2, especially (38). In this case, no additional constraint is required on the coefficients of compressor performance curve, but the curve $\gamma_o(A_e)$ defined by (26) may admit more than one extreme point. Incidentally for the compressor in [13], $K_{\min} = 7/9$ as well.

4 Numerical Simulations

The nonlinear feedback control law as presented in the previous section is tested in this section with numerical simulations. The compressor model as in [13] is used where various parameters are:

$$\lambda = 1.75, \quad H = 0.18, \quad W = 0.25, \quad B = 2, \quad a = 1/3.5,$$
$$c_0 = 8/3, \quad c_1 = 1.5, \quad c_3 = -0.5, \quad l_c = 8, \quad l_F = \infty.$$

Figure 5 shows four simulation plots in the absence of the feedback control law (24). Plot (a) is a bifurcation diagram of (A_e, γ) that illustrates the subcritical pitchfork bifurcation associated with the hysteresis loop in rotating stall where the solid line indicates stability and the dotted line illustrates instability. The bifurcation diagrams in (b) – (d) of Figure 4 are obtained from (a) of Figure 4 using the relations satisfied for steady equilibrium solutions. The hysteresis loop in (a) of Figure 4 clearly has adverse effects for using the throttle as control actuator. This is seen from the fact that the operating points (Ψ_e, Φ_e, A_e) are not single-valued functions of γ. Thus control strategies are difficult to work when rotating stall occurs. However after using the nonlinear feedback control law, the pitchfork bifurcation in (a) of Figure 4 is changed from subcritical into supercritical as shown in (a) of Figure 5. The bifurcation diagrams in (b) – (d) of Figure 5 show that the adverse effects resulting from hysteresis loop are eliminated, and (Ψ_e, Φ_e, A_e) are all single-valued functions of γ. Hence our goal stated in Section 1 is achieved.

We notice from (a) and (c) of Figure 5 that at the critical value of γ, small perturbations in throttle position may cause large variations in the amplitude of the disturbance flow and the pressure rise. This problem can be eliminated at the expense of using large gain K. Figure 6 shows the bifurcation diagrams of $K = 1.167$ that is 50% increase of the gain $K = 7/9$. But the improvement is significant. We would like to emphasize that Theorem 3.1 holds for $K > 1$, at least in the case $K < 1 + 1/\sqrt{5} = 1.4472$ as discussed in the previous section. Similarly, the stability results in Theorems 3.2 and 3.3 hold for $K \geq K_{\min}$ where $K_{\min}$ is given in (43). The effect of aggressive control gain ($K = 1.167$) is obvious from (a) and (c) of Figure 6. The critical value of γ_o is now about 0.4, 35% smaller than that of $K = 7/9$, thus increasing the tolerance for the disturbance in throttle.

5 Conclusion

A nonlinear control approach based on bifurcation theory was developed to design a feedback control law for rotating stall control in axial compressors. The proposed control system employed pressure rise as output measurement and throttle position as actuating signal. The proposed nonlinear feedback control law was shown to be effective in eliminating the hysteresis loop associated with rotating stall and in extending the stable operating range of the compressor characteristic. In comparison with the existing results on nonlinear control of rotating stall, our feedback control law accomplishes the same goal as those reported in [10, 16]. A more interesting problem is clearly whether or not the same feedback law

works for surge control that is currently under investigation.

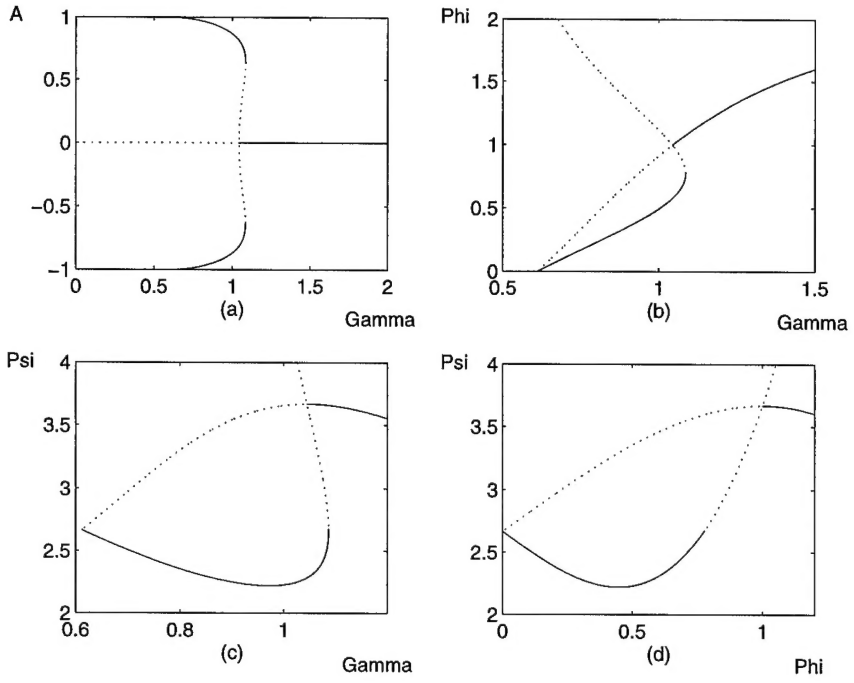

Figure 4: Bifurcation diagrams without feedback control

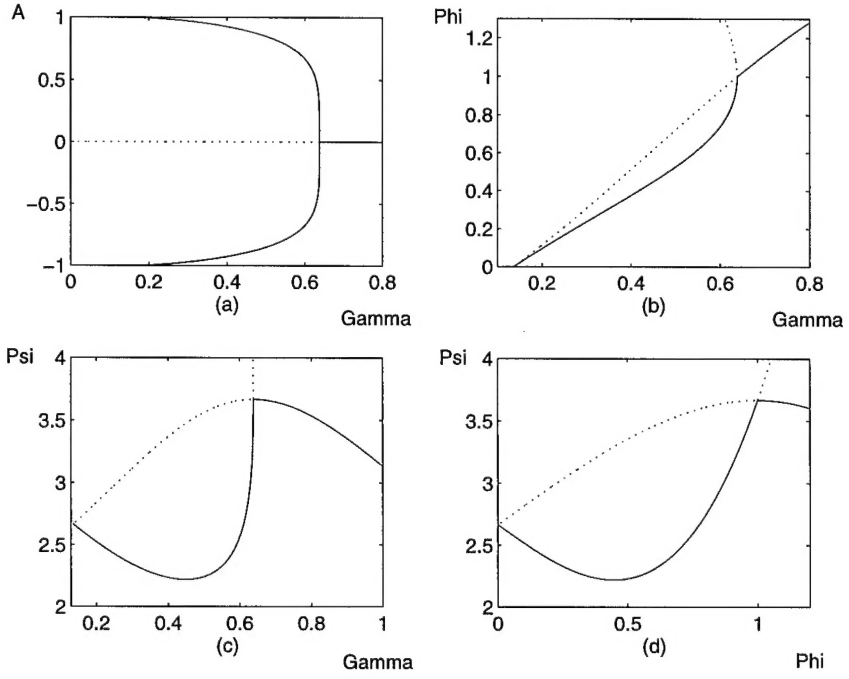

Figure 5: Bifurcation diagrams with feedback control

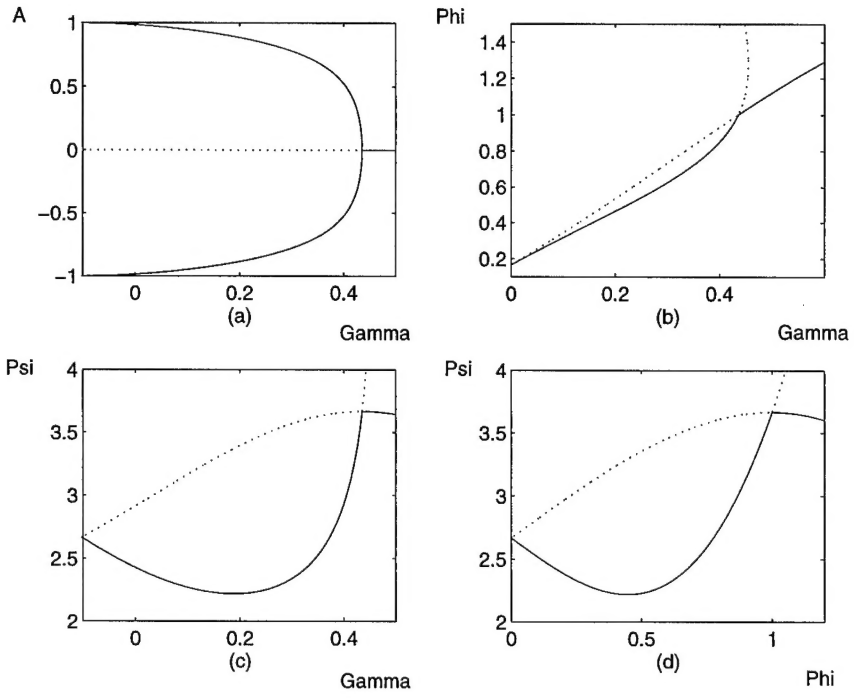

Figure 6: Bifurcation diagrams with large gain feedback control

Acknowledgement: The first author would like to thank his student Phillip Martin for his help in plotting all the pictures in this paper, and to AFOSR for the ASSERT Award that supports graduate study and research of Phillip Martin.

References

[1] R.A. Adomaitis and E.H. Abed, "Bifurcation analysis of nonuniform flow patterns in axial-flow gas compressors," in *1st World Congress of Nonlinear Analysis*, Aug. 1992.

[2] E.H. Abed, P.K. Houpt, and W.M. Hosny, "Bifurcation analysis of surge and rotating stall in axial flow compressors," *J. Turbomachinery*, vol 115, 817-824, Oct. 1993.

[3] O.O. Badmus, S. Chowdhury, E.M. Eveker, C.N. Nett, and C.J. Rivera, "A simplified approach for control of rotating stall – Part 1/2," in *29th Joint Propulsion Conference and Exhibit*, June 1993. AIAA Paper #93-2229/2334.

[4] R. D'Andrea, R.L. Behnken and R.M. Murray, "Active control of rotating stall using pulsed air injection: experimental results on a low-speed, axial flow compressor," in *SPIE Conference on Sensing, Actuation and Control in Aeropropulsion*, 1995.

[5] A.H. Epstein, J.E. Ffowcs Williams, and E.M. Greitzer, "Active suppression of aerodynamic instabilities in turbomachinery," *J. Propulsion*, vol. 5, 204-211, 1989.

[6] K.M. Eveker, D.L. Gysling, C.N. Nett and O.P. Sharma, "Integrated control of rotating stall and surge in aeroengines," in *SPIE Conference on Sensing, Actuation and Control in Aeropropulsion*, 1995.

[7] K.M. Eveker, D.L. Gysling, C.N. Nett and H.O. Wang, "Rotating stall and surge control," US Patent Application, US Serial Number 08355763, 1994.

[8] M.R. Feulner, G.J. Hendricks, and J.D. Paduano, "Modeling for control of rotating stall in high speed multi-stage axial compressors, in *ASME Gas Turbine Conference*, June 1994.

[9] G. Iooss and D.D. Joseph, *Elementary Stability and Bifurcation Theory*, Springer-Verlag, New York, 1980.

[10] D.-C. Liaw and E.H. Abed, "Active control of compressor stall inception: A bifurcation-theoretical approach," Technical Report, Institute for Systems Research, University of Maryland, 1992.

[11] F.E. McCaughan, "Bifurcation analysis of axial flow compressor stability," *SIAM J. Applied Mathematics*, vol. 20, 1232-1253, 1990.

[12] F.K. Moore and E.M. Greitzer, "A theory of post-stall transients in axial compressors: Part I – development of the equations," *ASME J. of Engr. for Gas Turbines and Power*, vol. 108, pp. 68-76, 1986.

[13] E.M. Greitzer and F.K. Moore, "A theory of post-stall transients in axial compressors: Part II – Application," *ASME J. of Engr. for Gas Turbines and Power*, vol. 108, pp. 231-239, 1986.

[14] J.D. Paduano, A.H. Epstein, L. Valavani, J.P. Longley, E.M. Greitzer, and G.R. Guenette, "Active control of rotating stall in a low-speed axial compressor," *J. Turbomachinery*, vol. 115, 48-56.

[15] S. Wiggins, *Introduction to Applied Nonlinear Dynamical Systems and Chaos*, Springer-Verlag, New York, NY, 1990.

[16] H.O. Wang, R.A. Adomatis and E.H. Abed, "Nonlinear analysis and control of rotating stall in axial flow compressors," in *American Control Conference*, 2317-2321, 1994.